Ruby at high pressure. III. A pumping scheme for the R lines up to 230 GPa

Jon H. Eggert, Fred Moshary, William J. Evans, Kenneth A. Goettel, and Isaac F. Silvera
Lyman Laboratory of Physics, Harvard University, Cambridge, Massachusetts 02138
(Received 13 November 1990)

We report on a B-line pumping scheme for exciting ruby R-line fluorescence which becomes useful above $\sim$100 GPa (100 GPa=1 Mbar). We have measured five ruby fluorescence lines in a quasihydrostatic-hydrogen-pressure medium to 230 GPa by using the most efficient argon-ion pump-laser wavelength at each pressure. The frequencies of the R and R' lines, as determined in the cubic-crystal-field approximation, shift linearly with the fractional volume change to the highest pressure reached. The R_1 and the R_3' lines remain thermalized and the oscillator strength of the R_3' line increases relative to the R_1 line to 230 GPa.

I. INTRODUCTION

The shift of the ruby R_1 line is widely used as a pressure scale in high-pressure diamond-anvil-cell (DAC) experiments.[1] Unfortunately, at pressures above $\sim$100 GPa, the fluorescence efficiency of the R_1 line decreases drastically.[2] Above about 150 GPa, measurements of ruby fluorescence in small 1–2-μm-diam ruby grains, which are desirable for pressure measurements in experiments on samples other than ruby, have been difficult or impossible to obtain. Even so, by using large amounts of ruby as a sample, there have been reports[3,4] of ruby-fluorescence lines excited with the 514- and 489-nm lines of the ruby laser to pressures in the 460–550-GPa pressure region, based on an extrapolated ruby scale.[5] The ruby scale has been calibrated to 180 GPa nonhydrostatically[5] and to 110 GPa quasihydrostatically.[6] However, if ruby fluorescence can be observed at very high pressures, the ease of pressure determinations based on the ruby-pressure scale provides a strong motivation to extend the calibrations of the pressure scale to higher pressures. Clearly, the extension of ruby-fluorescence measurements to the highest pressures now achievable and confidence in extrapolations of the pressure calibrations require an understanding of the ruby spectrum and fluorescence excitation mechanisms at high pressures. In this paper we shall draw strongly on the data and analyses presented in Refs. 7 and 2, referred to hereafter as papers I and II.

The electronic energy levels of ruby (Cr^{3+} in Al_2O_3) are well described by ligand-field theory.[9] The degenerate d-electron states of the Cr ion are split by the strong cubic crystal field (site symmetry O_h) into two d-electron eigenstates, t_{2g} and e_g. Small distortions of the octahedral Al site in Al_2O_3 give rise to a trigonal-field perturbation, which reduces the final site symmetry to C_{3v} and partially removes the electronic degeneracies. Spin-orbit coupling between the Cr ion and the d electrons also splits the degeneracies. In Fig. 1 we present a schematic energy-level diagram of ruby at 1 bar, showing the electron configuration in the t_{2g} and e_g states, the cubic-field terms, and the eigenstates after the trigonal-field and spin-orbit perturbations. In this paper, since we are only concerned with transitions to the ground state, we refer to the energy levels in the transition notation, shown in Fig. 1. Thus the $(t_2^3)^2E\bar{E}$ level will be referred to as the R_1 line, etc. In this notation the letter refers to the cubic-field approximation energy term and the subscripts refer to splittings caused by the trigonal and spin-orbit perturbations. We have also shown the approximate energies of each transition in Fig. 1.

The most common scheme for exciting the R-line fluorescence is electronic excitation of the U or Y bands, using a green or blue laser line. This excitation rapidly decays through nonradiative transitions to the R lines. Because of the rapid shift of the U and Y bands to higher

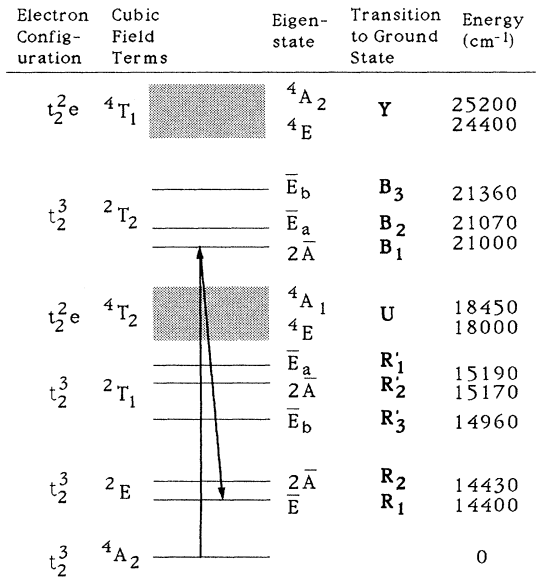

FIG. 1. Electronic energy levels of ruby. The cubic-field term levels are split by both trigonal-field and spin-orbit coupling perturbations. The arrow-headed lines denote our proposed new pumping scheme via the B lines. The standard pumping scheme is via the U or Y band. The approximate energies of the transitions at 1 bar are also given.

energy with increasing pressure, this pumping scheme becomes inefficient above 100 GPa, and the R_1-line fluorescence becomes weak and difficult to measure.[2,7] It has been proposed, based on calculations, that at very high pressures optical pumping through the B lines may become more efficient than through the U band.[2] We demonstrated that this is indeed the case. By selecting the appropriate pump wavelength at each pressure, we pumped the R lines by exciting the B lines at pressures between 118 and 230 GPa, based on extrapolation of the quasihydrostatic ruby scale. From the resulting fluorescence spectra, we measured the pressure shifts of the N_2, R_1, R_2, R'_3, and R'_{12} lines up to 230 GPa. Here N_2 refers to a satellite line due to crystal-field perturbations caused by fourth-nearest-neighbor Cr-ion impurities, and R'_{12} refers to the unresolved R'_1 and R'_2 lines.[7] We show that the R- and R'-line centers continue to shift linearly with the fractional volume change $\Delta V/V$ up to 230 GPA, and we give new fitting parameters[7] for Munro scaling theory.[10] We also demonstrate that the R_1 and R'_3 lines remain thermalized to 230 GPa, implying that the phonon coupling remains strong between these states. We find that the relative oscillator strength of the R'_3 to R_1 line increases with pressure up to 230 GPa.[7,8]

II. EXPERIMENTAL APPARATUS

The experiments on ruby discussed in this paper used a hydrogen-pressure medium[11] in a DAC and yielded quasihydrostatic ruby spectra. We loaded hydrogen cryogenically in a helium cryostat, as described by Silvera and Wijngaarden.[12] We used a modified Mao-Bell DAC,[13] a rhenium gasket,[4,14] and type-1A double-beveled diamonds.[14] Our diamonds had 50-μ central flat, 150-μm first bevel, and 300-μm second bevel diameters, with 6° first and 9° second bevel angles. We performed these experiments in the helium cryostat at temperatures between 77 and 195 K. At the highest pressures, about 20% of our sample area contained $\sim$1-μm-diam ruby grains (0.5 wt % Cr^{3+}) scattered at the edges of the $\sim$20-μm-diam sample. Based on measurements of various line splittings, the pressure on the ruby was classified as quasihydrostatic.[7] In addition, we determined our sample thickness by observing Fabry-Pérot fringes, due to multiple reflections between the aligned diamond-hydrogen-diamond interfaces.[11] Using the extrapolated refractive index of hydrogen,[15] we determined the thickness to be 2.3 μm at 230 GPa, and we observed no evidence of ruby bridging between the two diamond anvils. For all pressure determinations we used the quasihydrostatic pressure calibration,[6] corrected for low temperature.[11]

We excited ruby fluorescence with an argon-ion laser using the 4579-, 4658-, 4765-, 4880-, 4965-, 5017-, and 5145-Å laser lines. We used a microscope-spectrometer system mounted on a micrometer-resolution XYZ translation stage, as illustrated in Fig. 2. Ruby fluorescence was distinguished from pressure-induced diamond fluorescence, using the time-resolved chopping technique developed by Eggert, Goettel, and Silvera.[16] The fluorescence was dispersed with a 300-g/mm grating in an 18-cm spectrometer and detected by a 1024-element

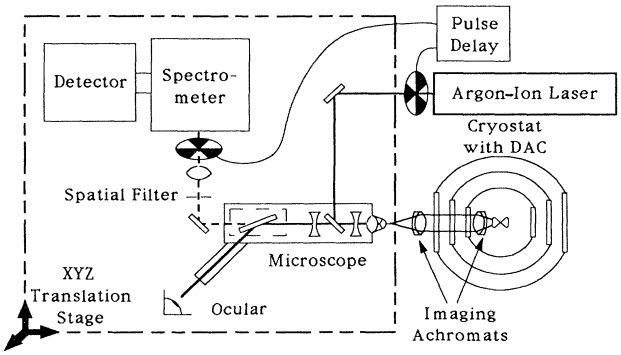

FIG. 2. Optical setup for measuring ruby fluorescence in a helium cryostat.

intensified diode array. Because of refractive effects, the windows of our cryostat limit the spatial resolution of a microscope by defocusing (even monochromatic) light. We solved this problem by inserting an achromatic lens inside the cyrostat with its focal point on the sample. In this way we collimated the light from the sample, which improved our spatial resolution. A second achromat formed a real image outside the cryostat, which we observed with our microscope. A spatial filter at the real image of the sample after the microscope allowed $\sim$5-μm spatial resolution of our sample.

III. RESULTS AND ANALYSIS

A. *B*-line pumping

The standard mechanism for exciting the R lines in ruby is to optically excite either the U or Y bands with a green or blue laser line. At high pressure the U and Y bands shift strongly to higher energies so that efficient pumping of the R lines requires progressively shorter-wavelength light. A calculation of the U-band absorption at three pump wavelengths was made in paper II as a function of pressure, using the experimental U-band shift and experimental parameters in a single-configuration-coordinate model. This calculation is replotted in Fig. 3(a) for 4880- and 4579-Å pump wavelengths. The R-line intensity should be proportional to the U-band absorption in the low power limit where the R-line intensity is determined by pump-laser absorption, rather than the R-line lifetime.[2] In Fig. 3(a) we also plot the experimental R_1-line intensity pumped at 4597 Å and at other, longer-wavelength laser lines which gave efficient R_1-line pumping. We see that for 4579-Å pumping, below 150 GPa, the experimental intensity follows the predicted absorption very well.

Ruby fluorescence has been excited conventionally by pumping with the 5145-, 4880-, and 4579-Å argon-ion laser lines. The calculation for U-band pumping shown in Fig. 3(a) suggested that, above 50 GPa, the most efficient R-line pumping should be achieved with the 4579-Å or shorter-wavelength line. At pressures above 150 GPa, this pumping scheme becomes very

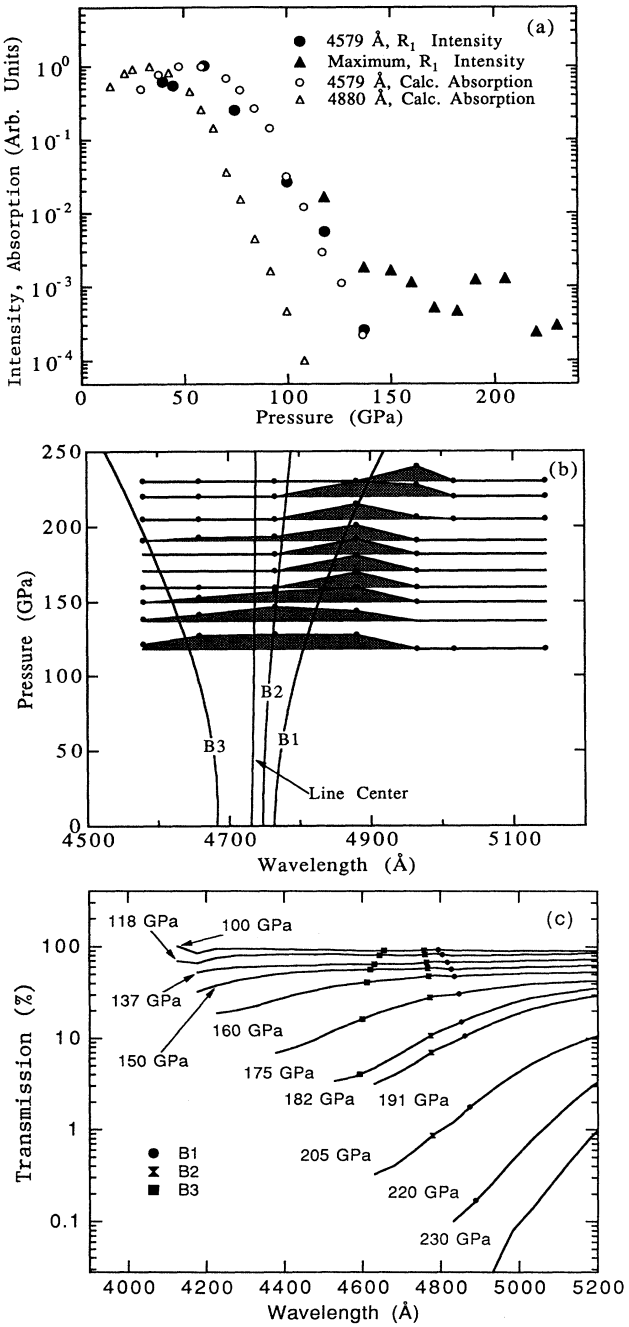

FIG. 3. Evidence for a new pumping scheme of the R lines via the B lines. (a) The calculated absorption in the U band, from paper II, for 4579- and 4880-Å light are shown by open circles and triangles, respectively. The solid symbols represent the experimental R_1-line intensity with 4579-Å pumping (circles) and with the most efficient longer-wavelength pumping at each pressure (triangles). (b) The predicted wavelengths of the B lines from paper I are given by the more or less vertical lines. The solid dots represent argon-ion laser lines which were used for pumping the ruby. The shaded curves denote the intensity of the R_1-line fluorescence, normalized to the most efficient pump wavelength at each pressure. The base lines of these curves are set at the pressure at which they were taken. (c) The transmission of diamond as a function of frequency for several pressures.

inefficient.[2,7,17,18] Since longer wavelengths pumped the U band less efficiently and shorter wavelengths were absorbed by the diamond anvils, ruby R-line fluorescence appeared to be limited in its useful pressure range. However, ruby fluorescence pumped with these laser lines has been reported in the 8120–8290-Å range, corresponding to pressures of 460 (Ref. 4) and 550 GPa,[3] by extrapolation of the nonhydrostatic pressure scale.[5] While there are large uncertainties in the use of the ruby-pressure calibration at these extreme pressures,[7,19] the ultrahigh-pressure ruby-fluorescence peaks[3,4] do not appear to be pumped by the standard U-band scheme. We shall show that, at pressures as low as 118 GPa, the conventional pumping scheme is not the most efficient one and that ruby fluorescence is not limited in its useful pressure range up to 230 GPa, even on micrometer-sized ruby grains. The pumping scheme which we describe also suggests an explanation for the observations of the very-high-pressure ruby fluorescence.[3,4]

In paper II it was suggested that the B lines might provide the most efficient pumping transition, at very high pressures. In Fig. 3(b) we show the predicted pressure dependence of the B-line wavelengths using the scaling theory fits given in paper I. These curves suggest that the B lines remain in the wavelength region of an argon-ion laser (indicated by the solid dots) up to very high pressure. We found that, by varying the pump-laser wavelength, the R lines were excited with differing efficiencies (indicated by the shaded curves). In agreement with the hypothesis of B-line pumping, the most efficient pump wavelength at high pressures varied with pressure and was not the 4579-Å line. Below 118 GPa we pumped with the 4579-Å line. Between 118 and 150 GPa we found that, in contrast to the U-band pumping scheme, the 4765-Å line gave the most efficient pumping. The 4880-Å line was most efficient between 160 and 220 GPa, and at 230 GPa, the 4965-Å line was best. These results are summarized in Figs. 3(a) and 3(b). In Fig. 3(a) we show the intensity of the R_1 line using the 4579-Å line (solid circles) and of the most efficient laser-pump wavelength as a function of pressure (solid squares). In Fig. 3(b) the solid circles represent measurements of the R_1-line intensity, normalized to the R_1-line intensity produced by the most efficient pump wavelength, at each pressure. The normalized intensity data are presented with the base line at each pressure corresponding to the measured pressure. The results shown in Fig 2(b) do not give a true picture of the relative efficiency of exciting with each laser line, due to the attenuation of the laser power by the stressed region of the diamond. In Fig. 3(c) we show the transmission as a function of wavelength which we measured for our diamond for several sample pressures.[11] For example, according to this figure, at 230 GPa, the laser power of the 4965-Å line is attenuated by more than two orders of magnitude.

At pressures below 150 GPa, where we observed R_1-line fluorescence with the 4579-Å laser line, the R_1-line intensity followed the predicted curve [open circles in Fig 3(a)] quite well. However, when we pumped with lower-energy laser ions at 118 GPa and above, the observed intensity clearly exceeded the intensity predicted for the

U-band pumping scheme. This, coupled with the narrow width of the peaked laser efficiency [Fig. 3(b)], leads us to conclude that we have observed R_1-line occurring through the B lines. The observed shift in the maximum pumping efficiency, shown in Fig. 3(b), qualitatively agrees with the prediction of the B-line shifts, although quantitatively the shift is larger than predicted. The apparent peak efficiency is strongly influenced by diamond absorption, shown in Fig. 3(c), at high pressure. Within these uncertainties we feel that the overall agreement with the B-line pumping mechanism is quite good.

The B-line extrapolation predicts that the 4579-Å line should efficiently pump the R_1 line near 200 GPa [Fig. 3(b)]. It is clear from Fig. 3(c) that large strain-induced absorption in our diamond anvils strongly attenuates the laser-pump power, resulting in apparent low pump efficiency. The strain-induced absorption in diamond anvils at very high pressures is not well understood and appears to vary drastically from experiment to experiment. This is supported by noting that in our experiment, at a pressure of 230 GPa, the transmission at 5400 Å had fallen to 10% and continued to decrease at shorter wavelengths.[11] In contrast, Vohra *et al.*[19] report that, in an experiment containing a sample of pure tungsten, at a pressure of 300 GPa, the transmission did not fall to 10% until about 4500 Å. Thus it appears that parameters such as type of diamond, diamond shape, gasket material, sample hole size, and sample material affect the position of the secondary absorption edge in diamond anvils at high pressure. Our hydrogen sample was thin (2.3 μm), and the diamond strain may have been quite high. In the solid gasket experiments yielding very large ruby-line shifts,[3,4] the lack of a soft sample may have led to thicker gaskets which lent better support to the diamond anvils so that they were under less strain.[4,13] B-line pumping could account for the ruby fluorescence observed in the ultrahigh-pressure experiments[3,4] if the diamond absorption at short wavelengths [pumped at 4579 Å (Ref. 4) and 4880 Å (Ref. 3)], was lower than in our experiment.

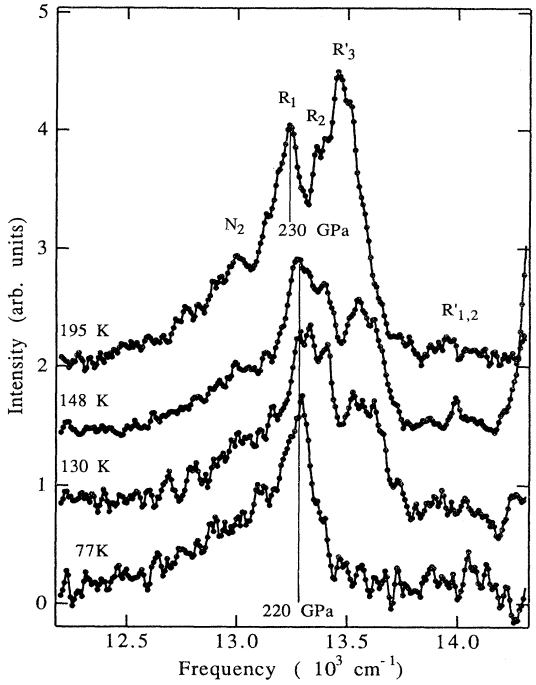

FIG. 4. Ruby fluorescence spectra near 220 GPa at various temperatures. These spectra were accumulated for 100 s and pumped with less than 100 mW of laser power.

B. Line shifts

We were able to measure the line shifts of the N_2, R_1, R_2, R'_3, and R'_{12} lines at several pressures when we warmed our sample about 100 K. In Fig. 4 we show ruby spectra near 220 GPa taken at temperatures between 77 and 195 K. The spectra shown in Fig. 4 were all accumulated for 100-s measurement times, using less than 100 mW of laser power; neither long accumulation times nor powerful laser excitations were necessary. During the warmup, the sample pressure rose from 220 GPa for the 77-, 130-, and 148-K scans, to 230 GPa for the 195-K scan. This pressure rise with increasing temperature is common and is probably due to thermal expansion in the DAC body.

By fitting the ruby spectra to a summation of five Gaussian line shapes, we obtained the frequency shifts with pressure, shown with earlier data[7] in Fig. 5. The long, low-frequency tail in Fig. 4 was modeled with an additional broad Gaussian centered near 13 000 cm^{-1} and was interpreted at arising from contributions due to phonon and neighbor-line sidebands. It was suggested in paper I that the splitting of the R'_{12} and R'_3 lines is characteristic of nonhydrostatic strain in ruby, since the trigonal perturbation is likely to be enhanced by nonhydrostatic strain, and the splitting is proportional to the square of the trigonal distortion. We see that the hydrogen sample at 230 GPa has similar hydrostaticity to the xenon-pressure medium (open circles in Fig. 5) at about

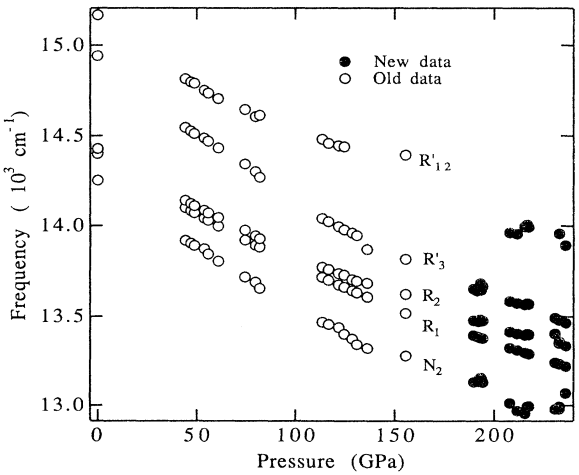

FIG. 5. Frequency shift of the fluorescence lines in this experiment, along with the shifts determined at lower pressures (paper I).

125 GPa. This is consistent with observations that hydrogen remains quasihydrostatic to very high pressures.[20] We note that, since the crossing of the R_3' line with the R lines is predicted to be due to nonhydrostaticity in the ruby (trigonal-field splitting), the expected crossing should occur at a higher pressure in a hydrogen pressure medium than in a xenon-pressure medium.[7]

Lower-pressure line shifts were fit in paper I using a scaling theory developed by Munro[10] and scaling linearly with $\Delta V/V$. Assuming that the cubic-field line-center frequencies shift linearly with $\Delta V/V$, the shifts are given by

$$\frac{\delta E}{E_0}=\frac{\delta V}{V}\left[\frac{5}{3}\beta+(2-\beta)\delta\Lambda+(1-5\beta)\delta\Omega\right], \qquad \beta=\left[\frac{(Dq)_0}{E_0}\right]\left[\frac{\partial E}{\partial Dq}\right]_0, \tag{1}$$

where E is the cubic line-center frequency, Dq is the cubic-field parameter, the subscript 0 refers to the 1-bar values, and δV and $\delta\Omega$ are adjustable parameters.[10] The values for β, given from the equations of Sugano, Tanabe, and Kamimura,[9] are $\beta(r)=0.0340$, $\beta(R')=0.0236$, $\beta(U)=1.000$, $\beta(B)=0.131$, and $\beta(U)=0.788$. The values of $\delta\Lambda$ and $\delta\Omega$ can be determined from experimental frequency versus pressure data for any two lines. In Fig. 6(a) we plot the line centers of the R and R' lines using a Birch-Murnaghan equation of state with $K_0=254$ GPa and $K_0'=4.3$.[21] We see that the line shifts are linear with $\Delta V/V$. A new fit to the Munro scaling theory is shown along with the previous fit in Fig. 6(b). We find that $\delta\Lambda=0.125$, and $\delta\Omega=0.035$, and the change in the fitting parameters is minor ($\delta\Lambda=0.129$, and $\delta\Omega=-0.051$ from paper I). The predicted extrapolations for the U, B, and Y lines differ only slightly from paper I and are not shown.

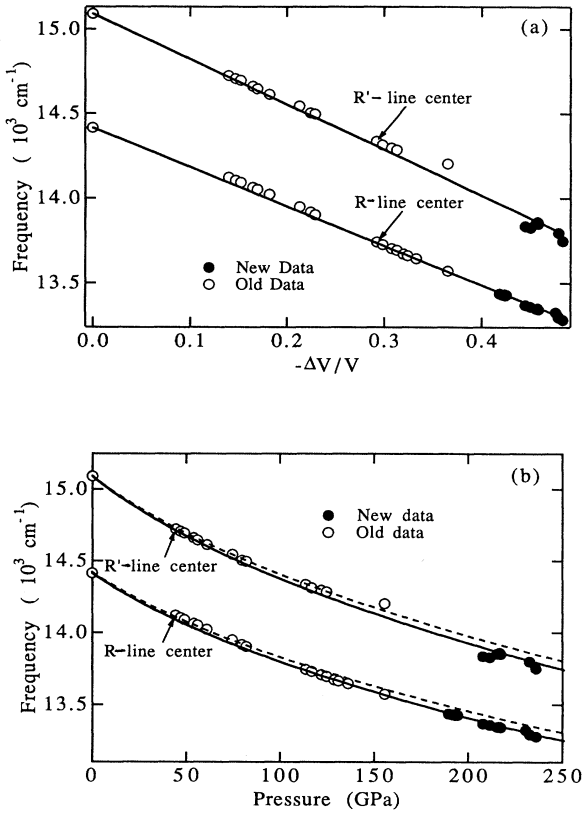

FIG. 6. Cubic-field line centers for the R and the R' lines. (a) The line centers shift linearly when plotted vs $\Delta V/V$. (b) The new fits for the parameters $\delta\Lambda$ and $\delta\Omega$ plotted vs pressure (solid lines) along with the fit determined in paper I (dashed lines).

C. Thermalization of lines

In Fig. 4 the R_3' line is seen to rise markedly in intensity with temperature. This is expected if, as at 1 bar, the R and R' lines are thermalized.[22] In this case the line intensities are given by a Boltzmann distribution

$$I_j=A\frac{f_j e^{-E_j/k_BT}}{\sum_i e^{-E_i/k_BT}}, \tag{2}$$

where I_j is the intensity of a given transition, A is a proportionality constant based on the pumping strength, f_i is the oscillator strength of a transition, E_i is the energy of an excited level, and T is the temperature. The intensity ratio of any two such transitions is given by

$$\frac{I_i}{I_j}=\frac{f_i}{j_f}e^{-(E_i-E_j)/k_BT}. \tag{3}$$

Specifically, for the R_1 and R_3' levels, we find

$$\ln(I)=\ln(f)-\frac{\Delta E}{k_BT},$$

where

$$I\equiv\frac{I_{R_3'}}{I_{R_1}}, \quad f\equiv\frac{f_{R_3'}}{f_{R_1}}, \quad \Delta E\equiv E_{R_3'}-E_{R_1}. \tag{4}$$

From our data we can measure I and ΔE, and we plot $\ln(I)$ vs $\Delta E/k_BT$ in Fig. 7(a). For thermalization the slope should be -1; we find slopes of $-1.30(6)$ for 190 GPa and $-1.24(17)$ for 220 GPa. We attribute the deviation in the slope from that for ideal thermalization to difficulties in determining contributions from unresolved lines (neighbor lines or phonon sidebands) to the R_1- and R_3'-line intensities. The linearity displayed in Fig. 7(a), along with the proximity of the fitted slope to -1, demonstrates that the R_1 and R_3' lines are probably thermalized up to 220 GPa.

For each spectrum the relative oscillator strength f of the R_3' and R_1 lines may be calculated from Eq. (4). In Fig. 7(b) we plot f versus pressure for our data and, for the lower pressure, data from paper I. Although there is substantial scatter in the data, the relative oscillator strength is seen to increase with pressure. The highest-pressure data, near 220 GPa, show an anomalously rapid

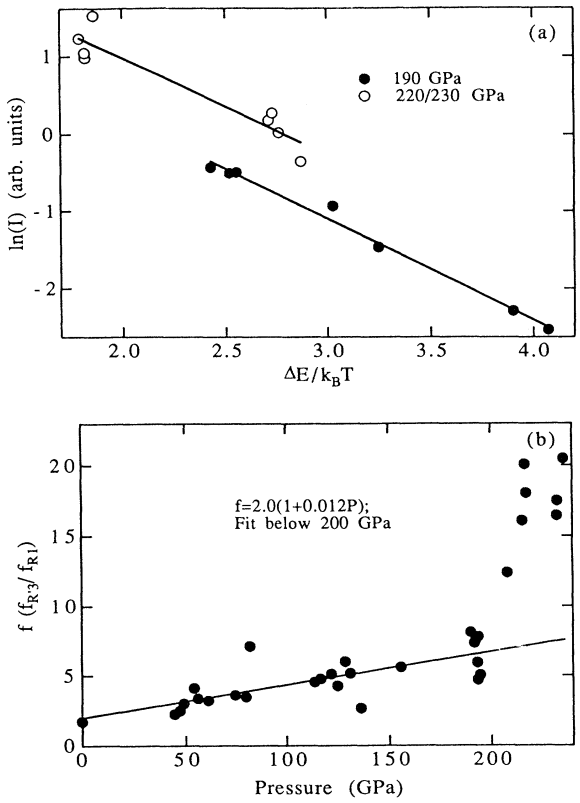

FIG. 7. (a) Plot of the relative intensity of the R_3' to R_1 lines as described by Eq. (4) in the text. (b) The relative oscillator strength of the R_3' to R_1 lines.

increase with respect to the lower-pressure values, and it would be interesting to study the relative oscillator strength to higher pressure. We note that the large values of f were observed in all of the spectra above 200 GPa, whether pumped with the 4880- or 4965-Å laser line. The observed increase in the relative oscillator strength with pressure is in contrast to a recent theoretical prediction[23] that $f^* \equiv f_{R'}/f_R$ should decrease as $(1/f_0^*)(\partial f^*/\partial P) = -3.7 \times 10^{-2}$. We find a best fit to our data, in the linear region below 200 GPa, of $(1/f_0)(\partial f/\partial P) = 1.2 \times 10^{-2}$. We note that our measurements compare the strengths of individual levels, split by the trigonal and spin-orbit perturbations, while the theoretical prediction was done in the cubic-field approximation.

IV. CONCLUSION

We have demonstrated that ruby R_1 fluorescence may be measured on micrometer-sized ruby grains to at least 230 GPa by choosing efficient pump wavelengths. Above 100 GPa the most efficient pump wavelength begins to shift to longer wavelengths, in contrast to the trend toward shorter wavelengths at lower pressures. We interpreted this to be due to a new pumping scheme for the R lines, occurring through B-line excitation. The R_1-line intensity, using B-line pumping, decreases much less rapidly than for U-band pumping and may continue to be viable to even higher pressures. The B-line pumping scheme may account for the reported ruby fluorescence at very high pressure.[3,4]

ACKNOWLEDGMENTS

We gratefully acknowledge financial support from the U.S. Air Force Astronautics Laboratory, Contract No. F04611-89-K-0003, and the Harvard Materials Research Laboratory, NSF Grant No. DMR-14003. One of us (W.J.E.) was also supported by the Fannie and John Hertz Foundation.

[1]J. D. Barnett, S. Block, and G. J. Piermarini, Rev. Sci. Instrum. **44**, 1 (1973).
[2]J. H. Eggert, K. A. Goettel, and I. F. Silvera, Phys. Rev. B **40**, 5733 (1989) (paper II).
[3]J. A. Xu, H. K. Mao, and P. M. Bell, Science **232**, 1404 (1986); Acta Phys. Sin. **36**, 501 (1987).
[4]W. C. Moss, J. O. Hallquist, R. Reichlin, K. A. Goettel, and S. Martin, Appl. Phys. Lett. **48**, 1258 (1986).
[5]P. M. Bell, J. A. Xu, and H. K. Mao, in *Shock Waves in Condensed Matter*, edited by Y. M. Gupta (Plenum, New York, 1986), p. 125.
[6]H. K. Mao, J. Xu, and P. M. Bell, J. Geophys. Res. **91**, 4673 (1986); R. J. Hemley, C. S. Zha, A. P. Jephcoat, H. K. Mao, and L. W. Finger, Phys. Rev. B **39**, 11 820 (1989).
[7]J. H. Eggert, K. A. Goettel, and I. F. Silvera, Phys. Rev. B **40**, 5724 (1988) (paper I).
[8]R. J. Hemley, H. K. Mao, and P. M. Bell, Trans. Am. Geophys. Union **67**, 1216 (1986).
[9]S. Sugano, Y. Tanabe, and H. Kamimura, *Multiplets of Transition-Metal Ions in Crystals* (Academic, New York, 1970).
[10]R. G. Munro, J. Chem. Phys. **67**, 3146 (1977).
[11]J. H. Eggert, F. Moshary, W. J. Evans, H. E. Lorenzana, K. A. Goettel, I. F. Silvera, and W. C. Moss, Phys. Rev. Lett. **66**, 193 (1991).
[12]I. F. Silvera and R. J. Wijngaarden, Rev. Sci. Instrum. **56**, 121 (1985).
[13]H. K. Mao and P. M. Bell, Carnegie Inst. Washington Yearb. **77**, 904 (1978).
[14]W. C. Moss and K. A. Goettel, Appl. Phys. Lett. **50**, 25 (1987); J. Appl. Phys. **61**, 4951 (1987).
[15]J. van Straaten and I. F. Silvera, Phys. Rev. B **37**, 1989 (1988).
[16]J. E. Eggert, K. A. Goettel, and I. F. Silvera, Appl. Phys. Lett. **53**, 2489 (1988).

[17]Y. K. Vohra, C. A. Vanderborgh, S. Desgreniers, and A. L. Ruoff, Phys. Rev. B **42**, 1989 (1991); J. H. Eggert, K. A. Goettel, and I. F. Silvera, *ibid.* **42**, 9191 (1991).

[18]S. J. Duclos, Y. K. Vohra, and A. L. Ruoff, Phys. Rev. B **41**, 5372 (1990).

[19]Y. K. Vohra, H. Xia, H. Luo, and A. L. Ruoff, Appl. Phys. Lett. **57**, 1008 (1990).

[20]H. E. Lorenzana, I. F. Silvera, and K. A. Goettel, Phys. Rev. Lett. **63**, 2080 (1989).

[21]R. E. Cohen, Geophys. Res. Lett. **14**, 37 (1987); A. P. Jephcoat, R. J. Hemley, and H. K. Mao, Physica B **150**, 115 (1988).

[22]S. Misu, J. Phys. Soc. Jpn. **19**, 2260 (1964); R. C. Powell, B. DiBartolo, B. Birang, and C. S. Naiman, Phys. Rev. **155**, 296 (1967).

[23]S. M. Sharma and Y. M. Gupta, Appl. Phys. Lett. **54**, 84 (1989).